Proceedings of NanoTech 2003, San Francisco, CA, Feb. 23-27, 2003.

Three-Dimensional, Full-Band, Quantum Modeling of Electron and Hole Transport through Si / SiGe Nano-Structures

[a,b]Cristian Rivas and [a]Roger Lake

[a]Department of Electrical Engineering, University of California, Riverside, CA 92521-0425
[b]Eric Jonson School of Engineering, University of Texas, Richardson, TX 75083

ABSTRACT

Si nanowires are direct gap with considerably heavier effective masses in both the conduction band and valence band compared to the bulk. Confinement leads to particularly rich structure in the valence band transmission versus energy functions. The single band model performs surprisingly well at calculating the effective band edges for the 1.54 nm wire. However, the accuracy of the single band calculation quickly becomes non-existent away from the band edge. The nanowire-bulk interface is an effective heterojunction with a band edge discontinuity corresponding to the confinement energies in the nanowire.

Keywords: Si nanowires, atomistic modeling, full-band modeling, quantum modeling, non-equilibrium Green functions.

1 INTRODUCTION

The scaling and miniaturization of CMOS has continued unabated, overcoming perceived technical obstacles ahead of schedule. It now appears that tunneling, the finite, countable number of electrons, and the random statistical fluctuations of dopants and alloys determine the ultimate limits of this trend. Modeling software should be developed now that can address the physics associated with Si-based device sizes at the ultimate quantum limit and to investigate nano-device concepts beyond traditional CMOS. Our objective is to develop a three-dimensional (3D), atomistic, full-band, full-quantum device simulator that can model electron and hole transport through strained, nano-scale Si-based structures. At this level, there is a natural merging of device and material simulations. The immediate 'device under test' is the 'self-assembled' Si / SiGe nanopillar. It consists of a core of SiGe within an oxidized Si nanowire. The oxidation process is self-limited at a certain radius of curvature [1], and the Ge is pushed ahead of the oxide front creating a Ge rich core [2]. Conversely one could envision starting with a relaxed SiGe virtual substrate resulting in SiGe leads with a highly strained Si quantum dot. To address the issues of electronic modeling and design of such structures, we have developed two different approaches both within the non-equilibrium Green function framework. This framework is described for a 1D planar system in [3]. The first approach is based on a three-dimensional (3D) discretization of the single-band effective mass equation. The second is based on the full-band $sp^3s^*d^5$ localized orbital model [4].

As a starting point, we have considered two types of structures, ideal, infinite Si wires passivated with H, and semi-infinite wires sitting on a planar Si substrate also passivated with H. Plan views and elevations of the wires are shown in Fig. 1. On the left is shown a H passivated Si ideal wire which in plan view is seen to be a 9x9 array of Si atoms with edges along the (110) and $(\bar{1}10)$ directions. The red atoms are Si and the blue atoms are H. For the infinite wires, we calculate both transmission and the E-k dispersion relations to determine effect of confinement on the position of the valley maximums and minimums and

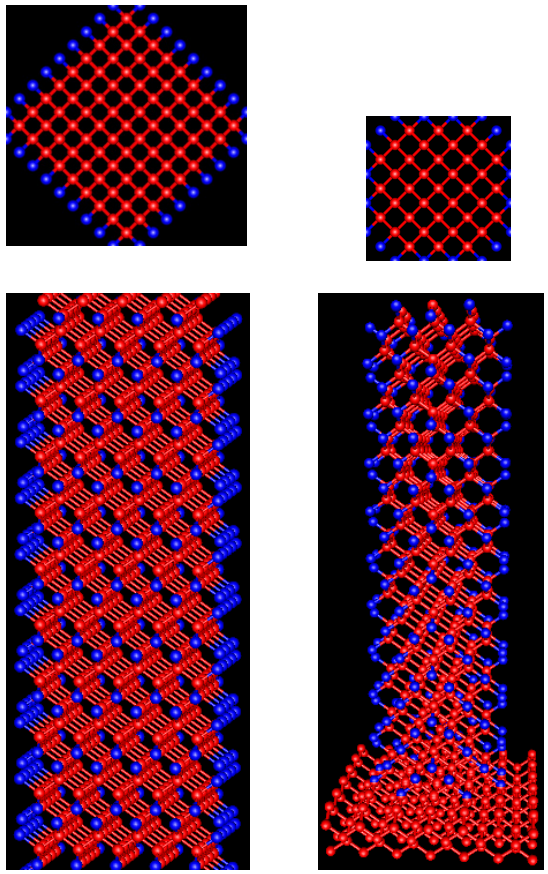

Fig. 1. Two types of Si wires considered. Left: ideal 1.54 nm x 1.54 nm Si wire. Right: 1.15 nm diameter Si wire on planar Si substrate. Si atoms in red and H atoms in blue.

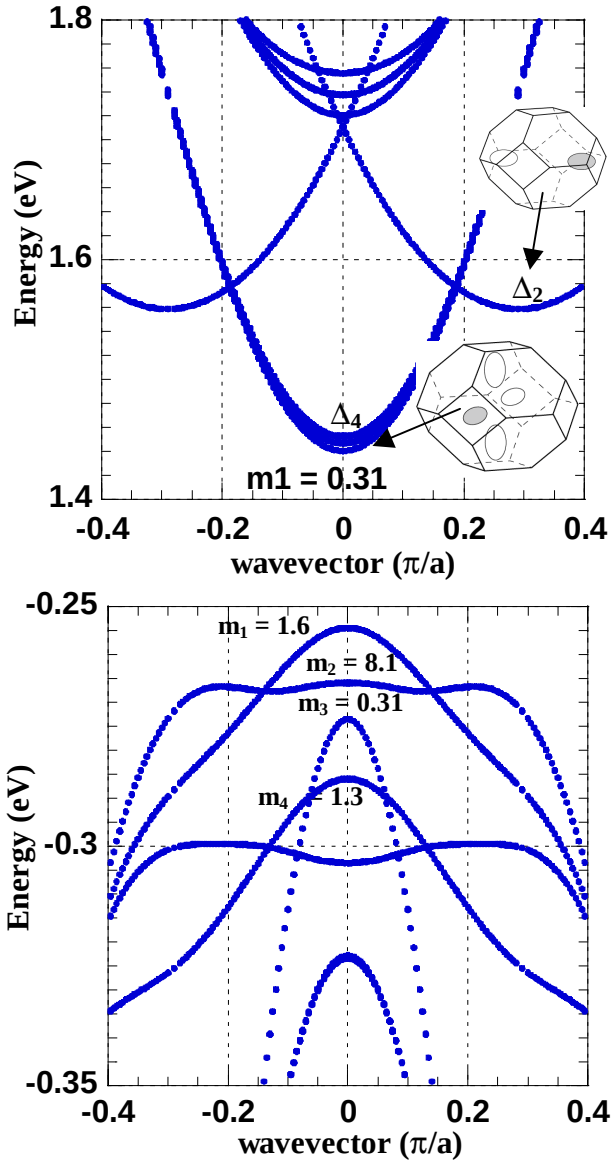

Fig. 2. E-k plots of conduction and valence band for 2.3nm square Si wire.

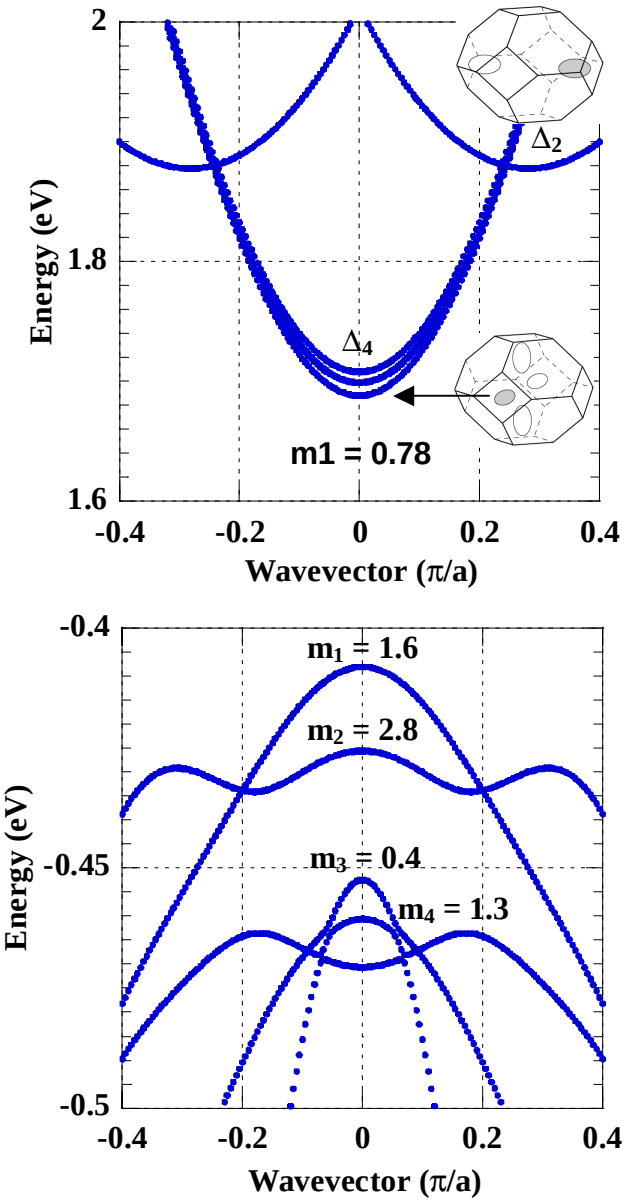

Fig. 3. E-k plots of conduction and valence band for 1.54 nm square Si wire.

their corresponding effective masses. The infinite wires as shown on the left are identical to the ones considered in [5] and our sp^3s^*d results quantitatively compare with theirs. We have also simulated wires standing on planar substrates as shown on the right of Fig. 1, and we compare transmission calculations of the wire on substrate versus those for the ideal wire.

2 BAND GAPS AND EFFECTIVE MASSES

The E-k diagrams of the conduction and valence bands for a 1.54nm square wire (9x9 Si atoms) and a 2.3 nm square wire (13x13 Si atoms) are shown in Figs. 2 and 3. They are calculated using the $sp^3s^*d^5$ model including spin-orbit coupling with matrix elements optimized using a genetic algorithm to give the correct T=300K bulk Si bandgaps and masses [6]. The unit cell of the 9x9 wire is shown in Fig. 4. The energy axis is such that 0 eV corresponds to the valence band edge of bulk Si.

The bandgaps of the 2.3nm and 1.54 nm Si wires are 1.76 and 2.1 eV, respectively, as compared to 1.12 eV of bulk Si. The band minimum in the conduction band is now at k=0 resulting from confinement of the 4 equivalent Δ valleys shown at the bottom right of the conduction band E-k plots. The conduction band masses of 0.31 for the 2.3 nm wire and 0.78 for the 1.54 nm wire are considerably heavier than the bulk transverse mass of 0.19 which is the mass along the wire axis in the Δ_4 valleys. The changes in the valence bands are just as large. For both wires, the mass of

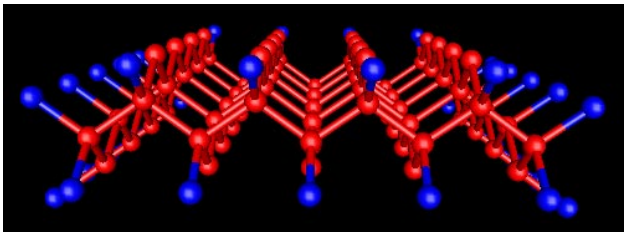

Fig. 4. Unit cell of the 1.54 nm wire.

the highest valence band is 1.6, which is 3.3 times heavier than the heavy hole mass of 0.49 for bulk Si. For the 2.3 nm wire, 4 bands lie within less than 2 $k_B t$ of the of the valence band edge with the second highest band almost flat with an effective mass of 8.1. The lightest mass of 0.31, which is 1.9 times the bulk light hole mass of 0.16, occurs for the third band 20 meV below the valence band edge.

3 COMPARISON WITH SINGLE BAND

One of our goals is to develop modeling capability suitable for device design of these nanoscale Si structures. A design tool requires fast modeling capability, which leads us to evaluate a discretized single band effective mass model for these structures. In the single band model we perform a calculation for each unique valley independently and then multiply the result by the valley degeneracy and a factor of 2 for spin. A comparison of the transmission coefficient calculated from the single band model and the full-band sp3s*d5 model for the 1.54 nm wire is shown in Fig. 5. The transmission coefficient initially jumps up to a factor of 8 at the conduction band edge that is formed by the 4 equivalent Δ_4 valleys each with 2 spin channels. What

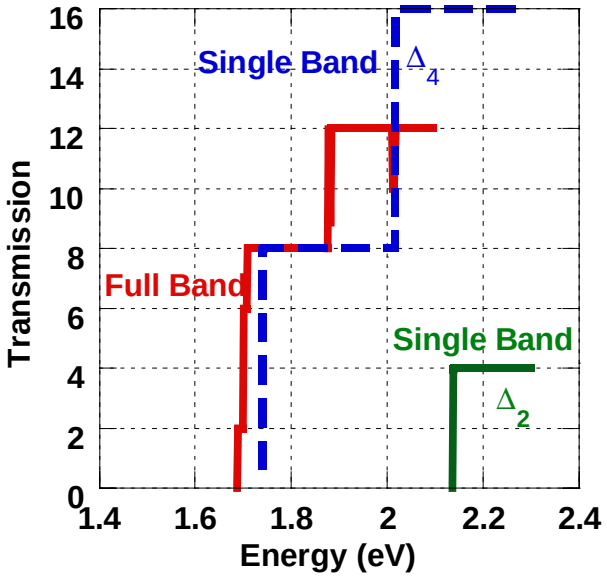

Fig. 5. Comparison of full-band and single band calculations of transmission coefficient through the 1.54 nm wire conduction bands.

is most interesting is that even for this extremely confined quantum wire, the conduction band edge predicted by the single band model is off by 50 meV which is only 9% of the total confinement energy predicted by the full band model of 0.58 eV. Of course the results quickly diverge at higher energies. The single band prediction of the Δ_2 edge is completely off. The second turn on in the full-band calculation is the result of the Δ_2 edge which gives rise to the step height of 4, 2 valleys times 2 spins. The single band calculation is off by 260 meV.

The valence band comparison shown in Fig. 6 cannot be made on the same plot. However, again, the difference in the predicted energy of the first turn-on, i.e. the effective band edge, is only 50 meV. Thus, if one is only interested

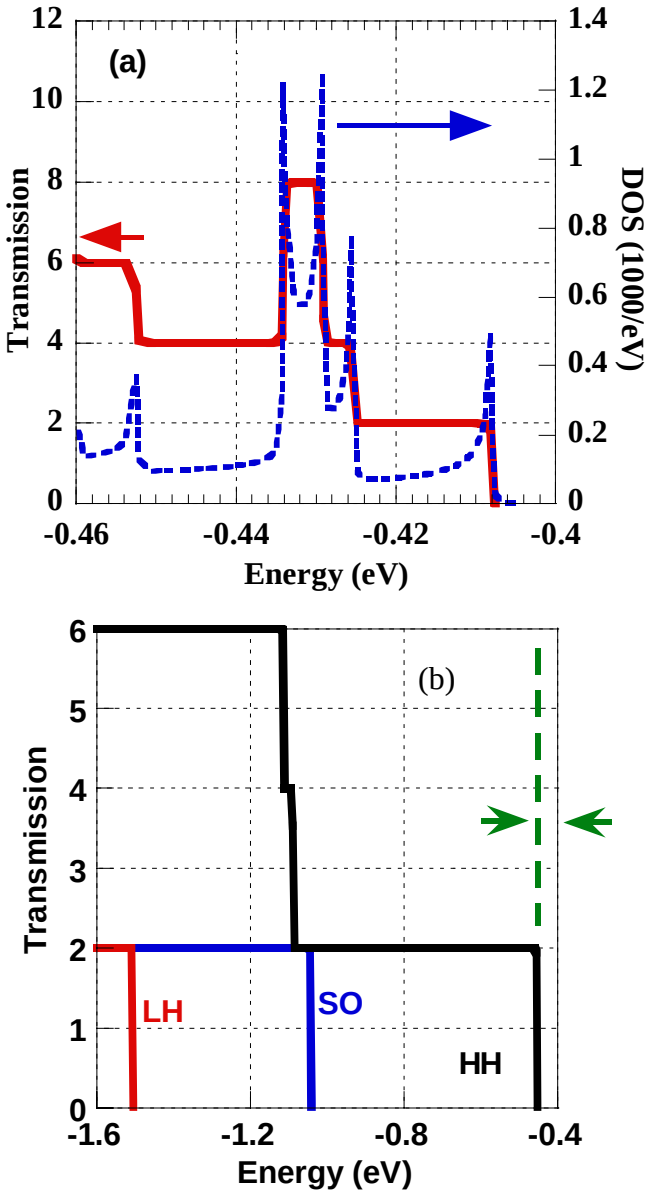

Fig. 6. Comparison of (a) full band and (b) single band calculated transmission coefficients through the 1.54 nm wire valence band.

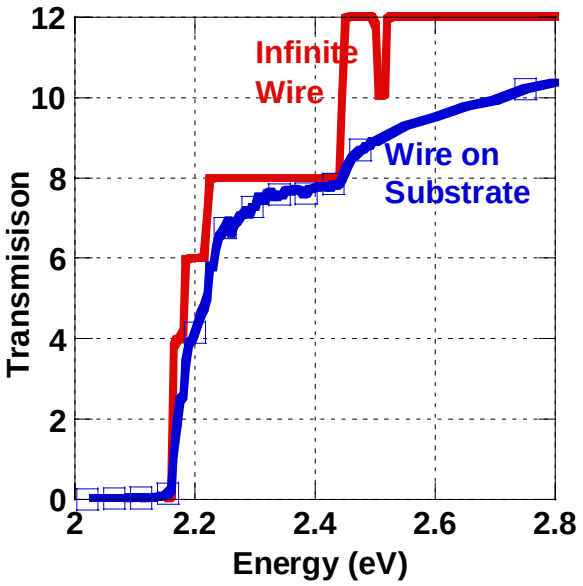

Fig. 7. Comparison of transmission through the wire shown on the right in Fig. 1 with injection from the substrate versus an ideal wire.

in the effective band edges resulting from confinement, a single band model is only off by approximately 10% even for these extremely quantized structures. But the results in the valence band diverge much more quickly, and the entire full band plot lies within the arrows on the single band plot. One interesting feature of the full band plot is the quick turn-on at –0.43 eV followed by a turn-off at –0.434 of a double channel. This results from the energy being scanned down through the second valence band of Fig. 3. Such a result could never result from a single band type calculation.

4 WIRE ON SUBSTRATE

So far, we have considered ideal infinite Si wires. However, actual wires stand on bulk planar substrates from which electrons are injected. Therefore, we have developed the capability to model Si wires with bulk planar contacts. The required 2D surface Green function is obtained by Fourier transforming the 1D planar orbital surface Green function described in [3] over the 2D Brillouin zone. The actual wire that we simulate is shown in Fig. 1 on the right. Fig. 7 shows a comparison of the calculated transmission coefficients for an ideal wire and a wire on a substrate. The difference can be understood if one considers the difference in the band edges of the wire and bulk. One effectively has a heterojunction at the wire – bulk interface and is then looking at injection over a barrier of 1 eV. Thus, reflection occurs in the bulk-wire system reducing the ideal plateaus in the transmission.

5 CONCLUSION

In conclusion, we have developed both continuum single-band and atomistic full-band 3D non-equilibrium Green function codes for modeling and design of Si / SiGe nanowires. The Si nanowires are direct gap with considerably heavier effective masses in both the conduction band and valence band compared to the bulk. Confinement leads to particularly rich structure in the valence band transmission versus energy functions. The single band model performs surprisingly well at calculating the effective band edges for the 1.54 nm wire. However, the accuracy of the single band calculation quickly becomes non-existent as one moves away from the band edge. The nanowire-bulk interface is an effective heterojunction with a band edge discontinuity corresponding to the confinement energies in the nanowire. This results in reflection and reduction of the transmission from the ideal plateaus.

ACKNOWLEDGEMENTS

This work was supported by the NSF NIRT grant DMR-0103248 and DOD/DARPA/DMEA under grant number DMEA90-02-2-0216. The computer simulations were performed on the UCR Institute of Geophysics and Planetary Physics (IGPP) Beowulf computer Lupin.

REFERENCES

1. H. I. Liu, D. K. Biegelsen, F. A. Ponce, N. M. Johnson, and R. F. W. Pease, Appl. Phys. Lett., **64**, 1383 (1994).
2. D. Nayak, K. Kamjoo, J. C. S. Woo, J. S. Park, and K. L. Wang, Appl. Phys. Lett., **56**, 66 (1989).
3. R. Lake, G. Klimeck, R. C. Bowen and D. Jovanovic, J. of Appl. Phys., **81**, 7845 (1997).
4. J. M. Jancu, R. Scholz, F. Beltram, and F. Bassani, Phys. Rev. B, **57**, 6493 (1998).
5. Y-J. Ko, M. Shin, S. Lee, and K. W. Park, J. Appl. Phys., **89**, 374 (2001).
6. G. Klimeck, R. C. Bowen, T. B. Boykin, C. Salazar-Lazaro, T. A. Cwik, and A. Stocia, Superlatt. Microst., **27**, 77 (2000).